Journal of Membrane Science 352 (2010) 222–230

Contents lists available at ScienceDirect

Journal of Membrane Science

journal homepage: www.elsevier.com/locate/memsci

Performance of a novel ZrO_2/PES membrane for wastewater filtration

Nermen Maximous, George Nakhla*, Wan Wan, Ken Wong

Department of Chemical and Biochemical Engineering, Faculty of Engineering, University of Western Ontario, 1151 Richmond Street, London, Ontario, Canada N6A 5B9

ARTICLE INFO

Article history:
Received 19 November 2009
Received in revised form 4 February 2010
Accepted 5 February 2010
Available online 13 February 2010

Keywords:
ZrO_2
Polyethersulfone
Fouling mitigation
Activated sludge
Wastewater

ABSTRACT

The membrane bioreactor (MBR) process has now become an attractive option for the treatment and reuse of industrial and municipal wastewaters. However, the MBR filtration performance inevitably decreases with filtration time due to membrane fouling. Over the past two decades, increased interests in improving the performance of filtration membranes (i.e., reducing membrane fouling) have encouraged the development of new classes of chemically modified membranes. In this study polyethersulfone (PES) membranes and membranes with five different weight ratios of ZrO_2 to PES of 0.01, 0.03, 0.05, 0.07 and 0.1, were prepared by the phase inversion method and applied to activated sludge filtration in order to evaluate their fouling characteristics. The membranes were characterized using field-emission scanning electron microscope (FESEM). The ZrO_2/PES membrane strengths were higher than those of the neat membrane. The membrane molecular weight cut-off (MWCO) and membrane thickness were slightly affected by the ZrO_2 addition. ZrO_2 entrapped membranes showed lower flux decline compared to the neat PES membrane, with fouling mitigation increasing with ZrO_2 particles content. The optimum load of ZrO_2 immobilized membranes for membrane bioreactor (MBR) application in terms of highest membrane permeability and lowest fouling rate was the 5% weight fraction of ZrO_2 with PES.

1. Introduction

The preparation of organo-mineral composite membranes with controlled properties has attracted attention recently. The formation of composite porous membranes by the addition of mineral fillers has been described in the literature for different applications such as gas separation, pervaporation nano- and ultrafiltration [1–4]. The modified membranes have the advantages of excellent separation performances, good thermal and chemical resistance and adaptability to the harsh wastewater environments [5,6]. Molinari et al. [5,6] investigated the use of TiO_2 nanoparticles in water purification. The fouling mitigation effects of immobilized TiO_2 UF membranes during the activated sludge filtration were investigated by Bae and Tak [7]. Recent studies of polyvinylidene fluoride (PVDF)-blending modifications have focused on blending the polymer with inorganic materials such as silica [8], Al_2O_3 [9] and some low molecular weight inorganic salts, such as lithium salts [10]. In our previous work [11], the effect of Al_2O_3 nanoparticles on the membrane fouling characteristics by activated sludge was studied by casting different weight ratios membranes of Al_2O_3 to polyethersulfone (PES) of 0.01, 0.03, 0.05, 0.1, and 0.2. The results showed that Al_2O_3 entrapped membrane had lower flux decline during activated sludge filtration compared to neat polymeric membrane.

Zirconia membranes are known to be chemically more stable than titania and alumina membranes, and therefore are more suitable for liquid phase applications under harsh condition [12]. Zirconia is also one of the common catalysts and hence it is a potential membrane material for high temperature catalytic reactions [13]. Furthermore in a comparative study, the toxicity of ZrO_2, as measured by IC50 concentration was higher than TiO_2 [14]. Guizard et al. [15] prepared ZrO_2 membranes, using a zirconium salt as precursor. The authors reported 85% retention of yellow acid (M = 759 g/mol). Vacassy et al. [16] used a polymeric sol–gel method to develop a ZrO_2 membrane on a commercial multi-channel support with a ZrO_2 ultrafiltration layer (MWCO support of 15 kDa), and observed 54% retention for saccharose (M = 342 g/mol) and 73% for Vitamin B12 (M = 1355 g/mol). Benfer et al. [17] used a polymeric sol–gel method using acetylacetone, diethanolamine or acetic acid as the modifier, to prepare a tubular ZrO_2 membrane, and observed 30% and 99% retention of orange G (M = 452 g/mol) and direct red (M = 991 g/mol), respectively. Dumon and Barmer [18] concluded that the presence of negatively charged phosphate or citrate groups at the surface of the ZrO_2 membrane (M6 Carbosep) prior to the ultrafiltration test favors a low adsorption of ovalbumin protein at pH 6.8–7.8. Zirconia micro-filtration membrane was also used after flocculation to treat oily wastewater [19]. The results showed that the membrane fouling decreased and the permeate flux and permeate quality increased with flocculation as pretreatment. Faibish and Cohen [20] developed a ceramic-supported polymer (CSP) zirconia-based ultrafiltration membrane and evaluated it for the filtration of synthetic anionic decane-in-water micro-emulsions

* Corresponding author. Tel.: +1 519 661 2111x85470; fax: +1 519 850 2921.
E-mail addresses: nmaximou@uwo.ca (N. Maximous), gnakhla@eng.uwo.ca (G. Nakhla), wkwan@eng.uwo.ca (W. Wan), khwong@uwo.ca (K. Wong).

0376-7388/$ – see front matter © 2010 Elsevier B.V. All rights reserved.
doi:10.1016/j.memsci.2010.02.021

with oil droplets in the size range of 18–66 nm. The membrane demonstrated fouling resistance even though it was completely wetted by the micro-emulsion solution and despite significant surface roughness of both the native and CSP membranes. Schaep et al. [21] casted a Zerfon® membrane using high polymer content (ZrO_2/polysulfone ratio of 80/20) in order to get denser membranes, closer to nanofiltration region with MWCO of 3200 Da. The filtration experiments carried out with different salts (Na_2SO_4, $CaCl_2$ and $MgSO_4$) showed that the ion retention in a salt mixture at 0.3 mequiv./l were 82%, 47%, 42% and 18% for SO_4^{2-}, Mg^{2+}, Na^+ and Cl^-, respectively.

Despite the aforementioned work on solute rejection of zirconia membranes [16–21] extensive literature search using SciFinder Scholar for zirconium oxide incorporation in membranes revealed few studies [22–24]. The aforementioned studies [22–24] confirmed the increased membrane permeability of ZrO_2 membranes. Moreover, no studies have been conducted on ZrO_2 immobilized PES membranes for sludge filtration and to fill this gap, this research aimed at preparing ZrO_2/PES membranes by introducing small amounts of ZrO_2 particles into the PES casting solution in order to improve the performance of PES membrane for wastewater filtration. Membrane structure was characterized by FESEM. The membrane strength, molecular weight cut-off (MWCO) and optimum ZrO_2 particles load were determined. The effect of ZrO_2 particles on biofilm attachment to membrane surface as represented by gel/cake layer formation and consequently the fouling mitigation effect of ZrO_2 particles was studied using activated sludge filtration.

2. Experimental

2.1. Membrane preparation

PES Radel A-100 (Solvay Advanced Polymers, Alpharetta, GA, USA) was used as the base membrane material. The membranes were prepared by the phase inversion method [25]. Zr(IV) oxide (Alfa-Aesar Canada Ltd.) 99% metals basis excluding Hf particles were used. The certificate of analysis provided by the supplier indicated the following composition (by weight): HfO_2 <3%, Fe_2O_3 of 0.006%, Cl^- of 0.0013%, SiO_2 of 0.004% and TiO_2 of 0.005%. Fig. 1 shows the ZrO_2 particles size distribution using Zeta Plus particle sizers (Brookhaven Instruments Corp, UK). The analysis was run for 5 times and the mean particle diameter was 221 ± 0.154 nm. It should be noted that particle followed a lognormal distribution with a 10th–90th percentile of 148–340 nm. Although the ZrO_2 particles were in the nanometer size range, the term nanoparticles has been avoided as it refers primarily to particles that are sized between 1 and 100 nanometers [26]. The 0.01, 0.03, 0.05, 0.07 and 0.1 ZrO_2/PES ratios (w/w) membranes were prepared by dispersing the ZrO_2 particles in N-methyl pyrrolidone (NMP) solution, after which the solutions were sonicated at 60 °C for 72 h to obtain uniform and homogeneous casting suspensions. Subsequently, 18 wt.% PES polymer was added and the mixture was sonicated again for a week. A 100 μm casting knife was used to cast the membranes onto a glass plate at room temperature. The nascent membrane was evaporated at 25 ± 1 °C for 15 s and then immersed in a deionized water coagulation bath maintained at 18 ± 1 °C for 2 min. To remove the remaining solvent from the membrane structure before testing, all prepared membranes were transferred to a water bath for 15–17 days at room temperature.

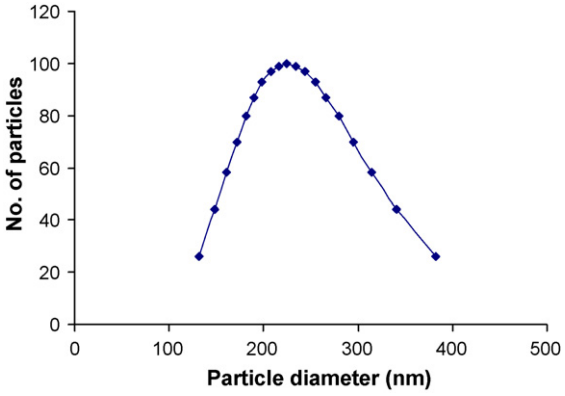

Fig. 1. ZrO2 particles size distribution.

2.2. Membrane characterization

The cross-sectional morphologies of the membranes were characterized using field-emission scanning electron microscopy (FESEM, Leo 1530, LEO Electron Microscopy Ltd.) at 1 kV with no conductive coating. The deionized water (DIW) flux was determined for the PES control membranes and the ZrO_2 entrapped PES at different trans-membrane pressures (TMPs) of 0.345, 0.69, 1.034, 1.38 and 1.724 bar. The maximum TMPs sustained by the membranes were determined by changing the TMP from 0.345 to 3.1 bar in increments of 0.345 bar using DIW. The TMP at which the membrane ruptured was taken as the maximum TMP sustained by the membrane. Molecular weight cut-off (MWCO) of the membrane was determined using 10% aqueous solutions of polyethylene oxide (PEO) (Acros Organics, USA) with Mw of 100, 200, 300 and 600 kDa. The concentrations of PEO were measured using LEICA Auto ABBE refractometer model 100500B (Letica Co., Rochester, MI, USA). Rejection was calculated by Eq. (1):

$$\%R = \left(1 - \frac{C_{per}}{C_{feed}}\right) \times 100 \quad (1)$$

where C_{per} is the concentration of PEO in permeate and C_{feed} is the concentration of PEO in the feed. The smallest molecular weight that is rejected by 90% is taken as the MWCO of the membrane [27].

2.3. Activated sludge

Activated sludge used in this study was cultivated in a submerged laboratory scale MBR (Fig. 2) treating synthetic wastewater for more than 8 months. Starch and casein, $(NH_4)_2SO_4$, and KH_2PO_4 were used as carbon, nitrogen and phosphorus sources, respectively. Additional nutrients and alkalinity ($NaHCO_3$) were also supplied to the reactor. The feed composition and the influent wastewater characteristics are summarized in Table 1 while Table 2 presents the activated sludge and effluent characteristics.

2.4. Membrane fouling analysis

Since the mode of constant TMP is suitable for the study of membrane fouling and is widely used for wastewater treatment [28–30], membrane filtration was carried out using a stirred batch cell operated under constant trans-membrane TMP (Model No. 8050, Amicon) as shown in Fig. 3. In order to alleviate the impact of compaction of the new polymeric membranes on flux, pre-filtration studies with pure deionized water (DIW) were conducted (8–10 filtrations) until a steady-state flux (J_{iw}) was achieved. For sludge filtration, the TMP and stirring speed were kept constant at 0.69 bar (as this is a typical TMP for submerged membranes like Zenon [31]) and 600 rpm, respectively. The permeate flux was determined by monitoring the volume of permeate with time. After the filtration test, the membrane was washed in a cross-flow manner with DIW and the pure DIW flux (J_{fw}) was measured 4 times after this cleaning

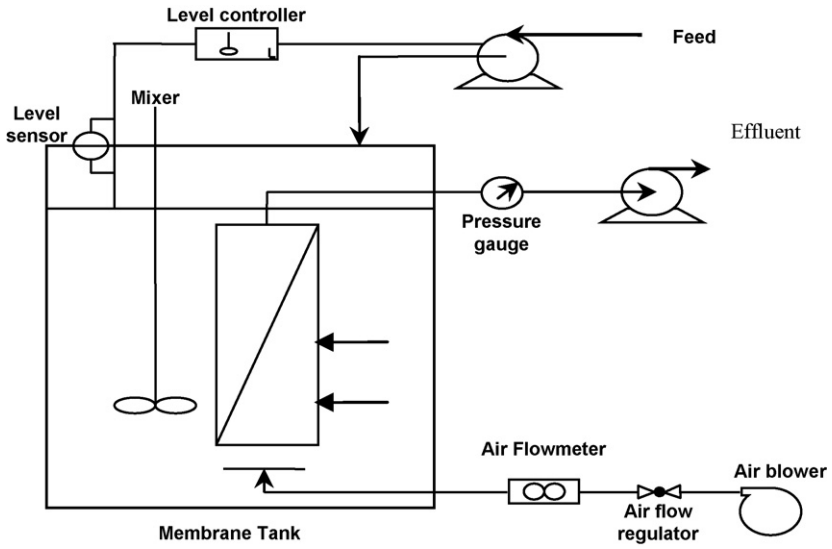

Fig. 2. Schematic diagram of MBR experimental setup.

Table 1
Feed composition and influent characteristics.

Feed compositions	
Compound	Concentration (mg/L)
Casein	125
Starch	84.4
Sodium acetate	31.9
$(NH_4)_2SO_4$	93.0
$MgSO_4{\cdot}7H_2O$	69.6
$CaCl_2{\cdot}2H_2O$	22.5
K_2HPO_4	5.9
NaOH	175.0
$FeCl_3$	11.0
$CuSO_4{\cdot}4H_2O$	0.08
$NaMoO_4{\cdot}2H_2O$	0.15
$MnSO_4{\cdot}H_2O$	0.13
$ZnCl_2$	0.23
$CoCl_2{\cdot}6H_2O$	0.42
KH_2PO_4	23.6
Na_2CO_3	216
$NaHCO_3$	169
Influent characteristics	
Parameters	Average ± SD (# of samples)
TSS (mg/L)	48.8 ± 9.8 (16)
TCOD (mg/L)	363.3 ± 33.5 (16)
NO_3 ($mgNO_3$-N/L)	0.2 ± 0.05 (16)
NH_3 ($mgNH_3$-N/L)	20.6 ± 4.3 (16)
PO_4 ($mgPO_4$-P/L)	6.1 ± 0.6 (16)

Table 2
Sludge and effluent characteristics.

Parameters	Sludge characteristics Average ± SD (# of samples)	Effluent characteristics Average ± SD (# of samples)
TSS (g/L)	8.1 ± 1.1 (24)	0.0 (6)
VSS (g/L)	5.9 ± 1.1(24)	0.0 (6)
SCOD (mg/L)	22.4 ± 2.0 (24)	6.7 ± 1.0 (24)
Turbidity (NTU)	6231 ± 846 (24)	<0.1
DOC (mg/L)	7.4 ± 0.7 (24)	2.2 ± 0.1 (24)
NO_3 ($mgNO_3$-N/L)	7.5 ± 1.6 (24)	7.4 ± 1.1 (6)
NH_3 ($mgNH_3$-N/L)	1.10 ± 0.57 (24)	0.9 ± 0.3 (6)
PO_4 ($mgPO_4$-P/L)	5.6 ± 1.3 (24)	5.4 ± 1.1 (12)
pH	7.3 ± 0.2 (24)	6.9 ± 0.1 (6)
DO	4.2 ± 0.8 (24)	NA

NA, not available.

regime. The degree of membrane fouling was calculated quantitatively using the resistance- in-series model [32].

$$J = \frac{\mathrm{TMP}}{\eta \cdot R_t} \tag{2}$$

where J is the flux (L/m^2 h), TMP is the trans-membrane pressure (0.69 bar), and η is the viscosity of water at room temperature.

$$R_t = R_m + R_f + R_c \tag{3}$$

Resistances values were obtained by the following equations:

$$R_m = \frac{\mathrm{TMP}}{\eta \cdot J_{iw}} \tag{4}$$

$$R_f = \frac{\mathrm{TMP}}{\eta \cdot J_{fw}} - R_m \tag{5}$$

$$R_c = \frac{\mathrm{TMP}}{\eta \cdot J} - (R_m + R_f) \tag{6}$$

where R_m is the intrinsic membrane resistance (i.e., the resistance due to membrane materials), R_f is the sum of the resistances caused by solute adsorption into the membrane pores or walls, and R_c is the cake resistance formed by cake or gel layer deposited over the membrane surface.

The membrane fouling rate was calculated by fitting the experimental data using Sigma Plot software version 10 (Systat Software, Inc., Canada). The calculated curves were generated by previous software; the data fit the exponential decay (3-parameters) equation (Eq. (7)) with R^2 of 0.90–0.99.

$$y = y^{\circ} + ae^{-bt} \tag{7}$$

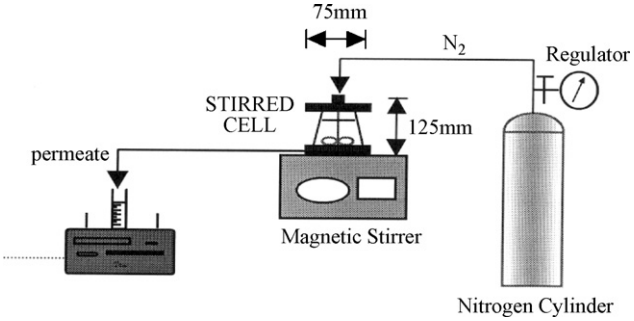

Fig. 3. Schematic diagram of stirred batch cell system.

where y is the permeability (L/m^2 h bar), t is the time (h), y° is the permeability at (t) equal infinity, and a and b are the regression constants. The fouling rate was determined using Eq. (8).

$$\frac{dy}{dt} = abe^{-bt} \tag{8}$$

The initial fouling rates (representing the initial curve) for all membranes are the averages of dy/dt at five points at times varying between 0.01 and 0.05 h. However, the final fouling rates are the averages of dy/dt at five points at times varying between 2.5 and 3 h.

3. Results and discussion

3.1. Membrane performances

The performance of the various membranes, as reflected by water quality parameter concentrations of both sludge and permeate, is presented in Table 2. It must be asserted that there were no observed performance differences between the PES and ZrO_2/PES membranes. As expected, the membranes removed suspended solids completely, affected 99.9% reduction of turbidity, 72% reduction of SCOD and DOC. A statistical analysis of the differences in ammonia, nitrates and phosphates between the raw sludge and filtrate indicated that observed differences were not significant at the 99% confidence limit. As expected, the performance of the membranes is consistent with that of ultrafiltration membranes. However, further confirmation of membranes ultrafiltration properties will follow below.

3.2. Membrane characterization

Fig. 4a–f shows the SEM pictures for the tested membranes. The pictures indicated that all prepared membranes were highly porous and asymmetric with sponge-like structures. Furthermore, the increased particle density of ZrO_2 in the 0.07 and 0.1 ZrO_2/PES membranes relative to the 0.01–0.05 ZrO_2/PES is quite evident. Table 3 shows the physical properties of the prepared membranes

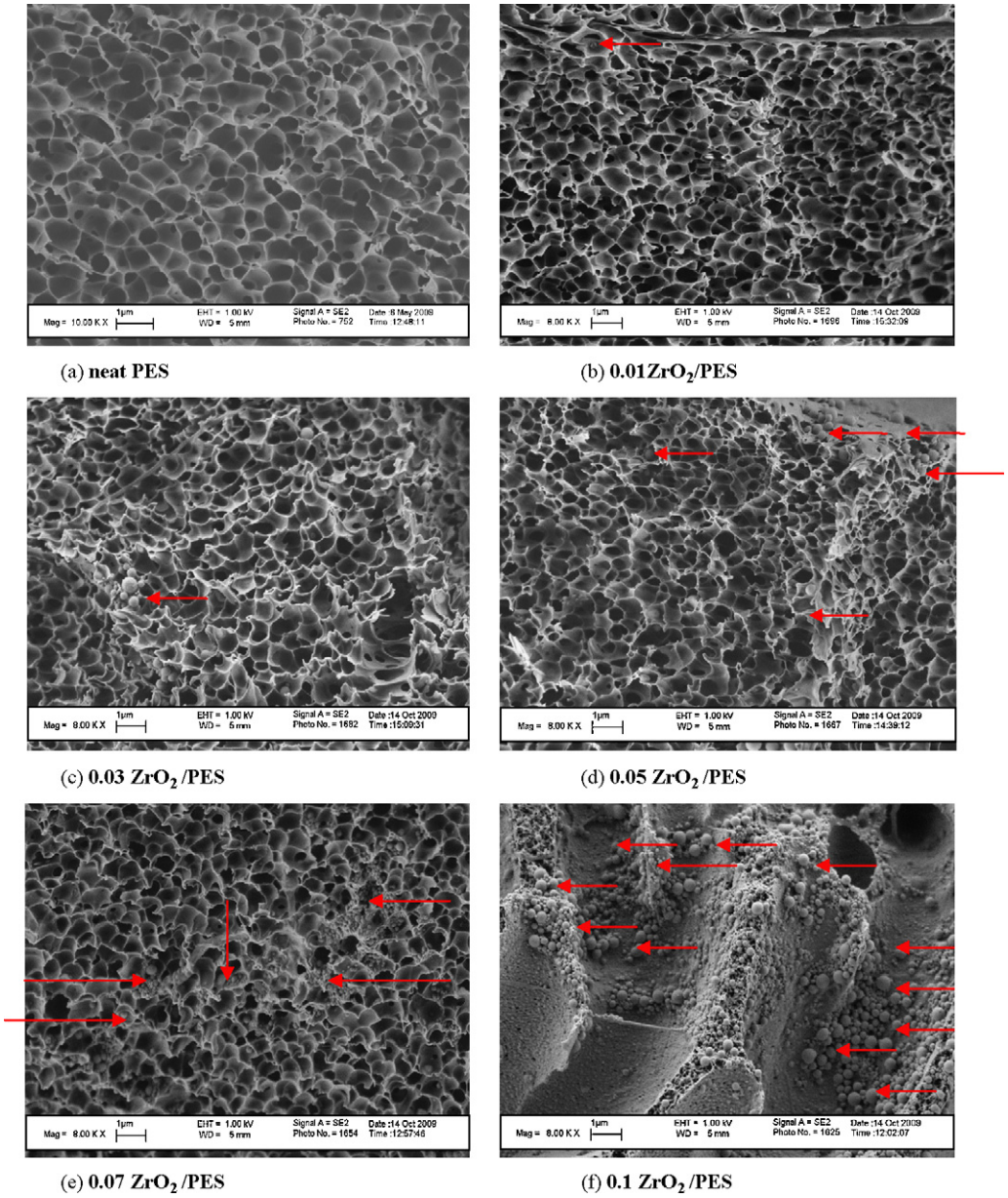

Fig. 4. SEM picture for the neat PES and ZrO_2/PES membranes: (a) neat PES, (b) 0.01 ZrO_2/PES, (c) 0.03 ZrO_2/PES, (d) 0.05 ZrO_2/PES, (e) 0.07 ZrO_2/PES and (f) 0.1 ZrO_2/PES

Table 3
Physical properties of ZrO_2/PES membranes.

ZrO_2/PES ratio	Membrane thickness (μm)	Particle density (particle/μm^2)	Maximum TMP (bar)	MWCO (kDa)
0.0 (control PES)	71.3 ± 1.4	0.0	1.724	600
0.01	76.4 ± 8.2	0.247	2.758	600
0.03	61.5 ± 6.9	0.368	2.758	600
0.05	62.3 ± 5.3	0.277	2.758	600
0.07	79.6 ± 3.3	0.494	2.758	600
0.1	73.2 ± 2.5	0.551	3.1	600

in terms of membrane thickness, particle density, maximum TMP and MWCO of the tested membranes using PEO. As expected the particle density per membrane unit area, Table 3, has increased with increasing the ZrO_2/PES ratio (except for 0.05 ZrO_2/PES membranes, which have a particle density of 0.277 particle/μm^2). It should be noted that the particle densities were computed using ImageJ software (U.S. National Institutes of Health, Bethesda, MD, USA). Comparison of the particle densities in the 0.07 ZrO_2/PES and 0.1 ZrO_2/PES membranes (Table 3) in conjunction with the SEM (Fig. 4e and f) with the rest of the membranes emphatically highlights the increased potential for pore clogging by ZrO_2 particles as reflected by particle densities ranging from 0.49 to 0.55 particle/μm^2 for the 0.07 and 0.1 ZrO_2/PES membranes, respectively, in contrast to 0.25–0.37 for the other three ZrO_2 loads. This observation is further supported by the increase in ZrO_2 particles size to 400 nm in 0.1 ZrO_2/PES membranes (Fig. 4f) in contrast to the 200 nm shown for the other ZrO_2/PES membranes (Fig. 4b–e), possibly due to particles agglomeration. As apparent from Table 3, the MWCO of the control PES was not affected by the addition of ZrO_2 particles; however, the particles effect on the membrane strength has been reflected by the higher maximum TMP sustained by ZrO_2/PES membranes. The MWCO is an established method to measure the pore size as the comparison with crystal structures and electron micrographs indicated that the membrane pore radius, *Rp*, is close to the effective hydrodynamic radius of the polymer in solution, *Rh*, of the largest PEG or PEO able to diffuse through the pore or to block ion conductance [33–35]. Lee et al. [36] plot the molecular weight (Mw) dependence of radius of gyration (*Rg*) for PEO, and linear fits yield the coefficient ν in $Rg \propto Mw^{\nu}$ equal to 0.515 within statistical error. According to the authors [36] the relation between the polymer Mw and *Rg* is presented by the following equation:

$$\log Rg = n \log Mw \quad (9)$$

where Mw of the polymer is in Da and *Rg* is in Å

The authors indicated that PEO behaves as an ideal chain. For high molecular weight polymers in "good solvents" (such as water for PEO), mean field and renormalization group treatments of excluded volume interactions yielded ν of 0.6 and 0.588, respectively [37]; a ν of 0.583 has been experimentally determined for PEO in water for 80,000 <Mw < 10^6 [38]. The polymer theory [39] predicts for a random coil polymer in a θ solvent (i.e., an ideal random flight chain) that:

$$Rh = 0.665\, Rg \quad (10)$$

Using Eqs. (9) and (10), the value of *Rh* for the PEO polymer (Mw = 600 kDa) and consequently the values of *Rp* of the tested membranes with MWCO of 600 kDa were estimated to be in the range of 629 Å (0.06 μm) based on ν of 0.515 [35] and 1554 Å (0.15 μm) based on ν of 0.583 [38]. Since the typical pore size range of ultrafiltration membranes is 0.01–0.1 μm [40], the results further confirm the ultrafiltration characteristics of the tested membranes.

Table 3 also shows that the membrane thickness increased slightly with the addition of ZrO_2 particles (except for 0.03 and 0.05 ZrO_2/PES, which have membrane thickness of 61.5 and 62.3 μm, respectively). This observation may suggest that the viscosity of the casting solutions and consequently their spreading on the glass plate during the phase inversion process have been slightly affected by the ZrO_2 particles addition. Table 4 shows the effects of the membrane physical characteristics on the membrane performances as reflected by different statistical correlations factors (*R*). As expected a good direct correlation (*R* = 0.88) was observed between the membrane DIW permeability and membrane steady-state permeability during sludge filtration. Maximum TMP linearly increased with ZrO_2 particle density (*R* = 0.89). A good positive correlation with *R* of 0.81 was observed between membrane thickness and its fouling resistance (R_f), a good inverse correlation (*R* = 0.78) between ZrO_2 particle density and membrane steady-state fouling rate and a strong inverse correlations with *R* of 0.99 and 0.90 between maximum TMP sustained by the membrane on one hand and membrane steady-state fouling rate and cake resistance (R_c) on the other hand, respectively.

3.3. ZrO_2-content

The effect of ZrO_2 particles concentrations on membranes DIW permeations is shown in Fig. 5. The values presented in this figure are the slopes of the straight lines generated by recording the DIW flux at different TMPs (0.345, 0.6895 and 1.0342 bar) with R^2 values of 0.89–0.99. The *Y*-error bars represent the 95% confidence intervals. As apparent from the figure, membrane DIW permeability increased with the increase in ZrO_2 particles loading and reached a maximum of 1580 L/m^2 h bar between the 0.03 and 0.05 ZrO_2/PES loads after which a significant decline was observed. The maximum DIW permeability for the 0.05 ZrO_2/PES of 1581 L/m^2 h bar is 1.8 times that of the PES. Since ZrO_2 as other metal oxides has higher affinity for water than PES, the penetration velocity of water into the nascent membrane increased with ZrO_2 concentration during the phase inversion preparation process. In addition, solvent diffusion from the membrane to the water can also be increased by ZrO_2 addition. Since the interaction between polymer and solvent molecules decreased due to the hindrance of ZrO_2 particles [41], solvent molecules could diffuse more easily from the polymer matrix resulting in an increase in the porosity of ZrO_2 entrapped membranes. On the other hand, the high concentrations of ZrO_2

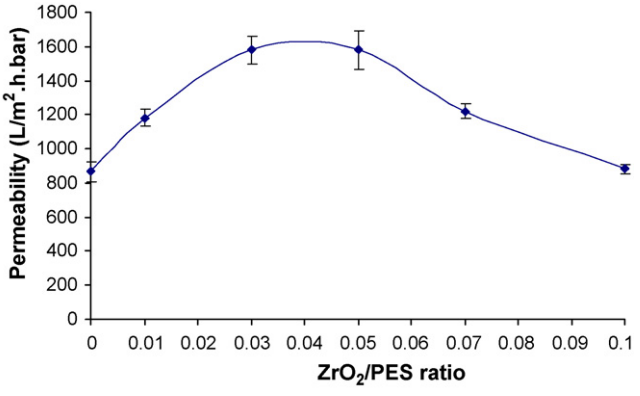

Fig. 5. The effect of ZrO_2 concentration on the membrane DIW permeation.

Table 4
Statistical correlations factors (R) between membrane physical characteristics and membrane performances.

	Membrane thickness	Particle density	Maximum TMP	Steady-state fouling rate	Steady-state permeability	R_t	R_c	R_f	DIW permeability
Membrane thickness	1								
Particle density	0.20	1							
Maximum TMP	0.01	**0.89**	1						
Steady-state fouling rate	0.04	**−0.80**	**−0.96**	1					
Steady-state permeability	−0.36	0.25	0.50	−0.69	1				
R_t	−0.23	−0.60	−0.77	**0.89**	−0.73	1			
R_c	0.20	−0.70	**−0.90**	**0.97**	**−0.83**	**0.86**	1		
R_f	**0.81**	0.14	0.12	−0.23	0.13	−0.61	−0.13	1	
DIW permeability	−0.65	0.13	0.34	−0.55	**0.88**	−0.50	−0.68	−0.12	1

The bold values highlight the good and strong correlations.

particles (i.e., 0.07 and 0.1 ZrO_2/PES) may clog some of the membrane pores in the phase inversion process leading to a decrease in the water flux.

3.4. Membrane fouling evaluation

3.4.1. Flux decline

The temporal flux declines for PES and ZrO_2 entrapped PES membranes using sludge as a feed at 20 °C and TMP of 0.69 bar are shown in Fig. 6. The figure shows that the ZrO_2 entrapped membranes have higher initial fluxes than the PES membrane. Results presented in this paper correspond to an average of two to four replicates with the membranes tested, randomly chosen from different independent sheets. It is important to emphasize that all the observed differences between the six different membrane fluxes were statistically significantly at the 95% confidence level. These results are consistent with the findings of Bae and Tak [42], who found that TiO_2 entrapped PES membranes showed higher flux for sludge filtration than neat polymeric membrane and with our previous work [11], which concluded that Al_2O_3 entrapped membrane showed lower flux decline during activated sludge filtration compared to neat polymeric membrane.

Fig. 7a–f illustrates the experimental and calculated permeability data, based on Eq. (7), for the membranes tested sludge filtrations. As apparent from the graphs, the permeability data are consistent with the hypothetical three-phase-process [43], comprised of initial fouling (phase 1) resulting in a rapid permeability decline mainly due to the irreversible deposition of the soluble fraction of the biomass suspension (presumably soluble microbial products, SMP), followed by deposition of sludge particles on the membrane surface and in the previously deposited layers is the main phenomenon occurring during phase 2 when the flux declines more slowly. Phase 3 is then defined when flux appears to stabilize, indicating that permeation drag and back transport have reached equilibrium. Although reduced permeation drag limits further severe fouling, compaction of the cake layer would play a significant role in the slight increase in filtration resistance observed during this last phase. As little fouling still occurs during phase 3, this operation can be maintained during a certain filtration period, before cleaning of the membrane is required [43]. Table 5 shows the initial and final fouling rates for sludge filtrations by the tested membranes as well as the steady-state permeability (y°) values. It is noteworthy that all the observed differences in fouling rates between the two phases for each membrane were statistically significantly at the 95% confidence level. Furthermore, the observed differences between the initial fouling rates as well as the steady-state fouling rates for all tested membranes were statistically significant at the 95% confidence level except for the differences between 0.01 and 0.03 ZrO_2/PES membranes.

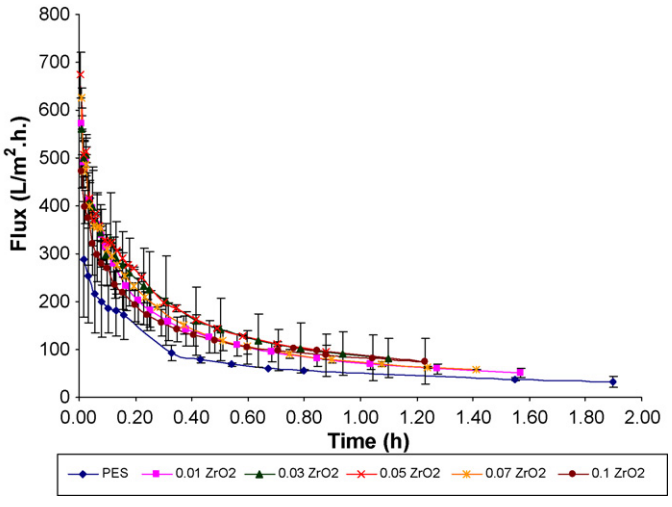

Fig. 6. Temporal flux decline for sludge sample at 0.69 bar.

As apparent from Table 5, despite the higher initial fouling rate, the steady-state fouling rates of ZrO_2 entrapped membranes were significantly lower (by 214, 184, 562, 135 and 481 times for 0.01, 0.03, 0.05, 0.07 and 0.1 ZrO_2/PES membranes, respectively) than the neat PES membrane. It is well known that membrane fouling can be influenced by hydrodynamic conditions, such as permeation drag and back transport, and chemical interaction between foulants and membranes [44–46]. Since all the membranes were tested at the same hydrodynamic condition, the different fouling behaviors could only be attributed to surface properties of the entrapped ZrO_2 particles in the membranes. The higher pseudo-steady-state permeability (Table 5) observed for the ZrO_2 entrapped membrane (3–10 times higher) than the neat membrane suggests that the surface of ZrO_2 entrapped membrane can be more hydrophilic than the neat polymeric membrane due to the higher affinity of metal oxides to water [7,11]. Therefore, hydrophobic adsorption between sludge particle and ZrO_2 entrapped membrane was reduced. Preliminary SEM data (Fig. 4b–f) confirmed the localization of particles near the membrane surface.

3.4.2. Fouling mitigation of ZrO_2 entrapped membranes

The various filtration resistances for different membranes, shown in Fig. 8, reflect the impact of ZrO_2 particles addition on PES membrane performance with the differences between membrane resistances (R_m) statistically insignificant at the 95% confidence level except for 0.1 ZrO_2/PES membranes. The R_m value for 0.1 ZrO_2/PES membranes was 1.3 times that of the neat membrane which suggests that the high load of ZrO_2 particles (Table 3) increased the membrane intrinsic resistance mainly due to the ZrO_2 particles aggregation. Insignificant differences between R_f values at the 95% confidence level were observed between membranes with ZrO_2 load of 0.03 up to 0.1. However, all the R_f values for all tested ZrO_2/PES membranes, ranging from 0.59×10^7 m^{-1}

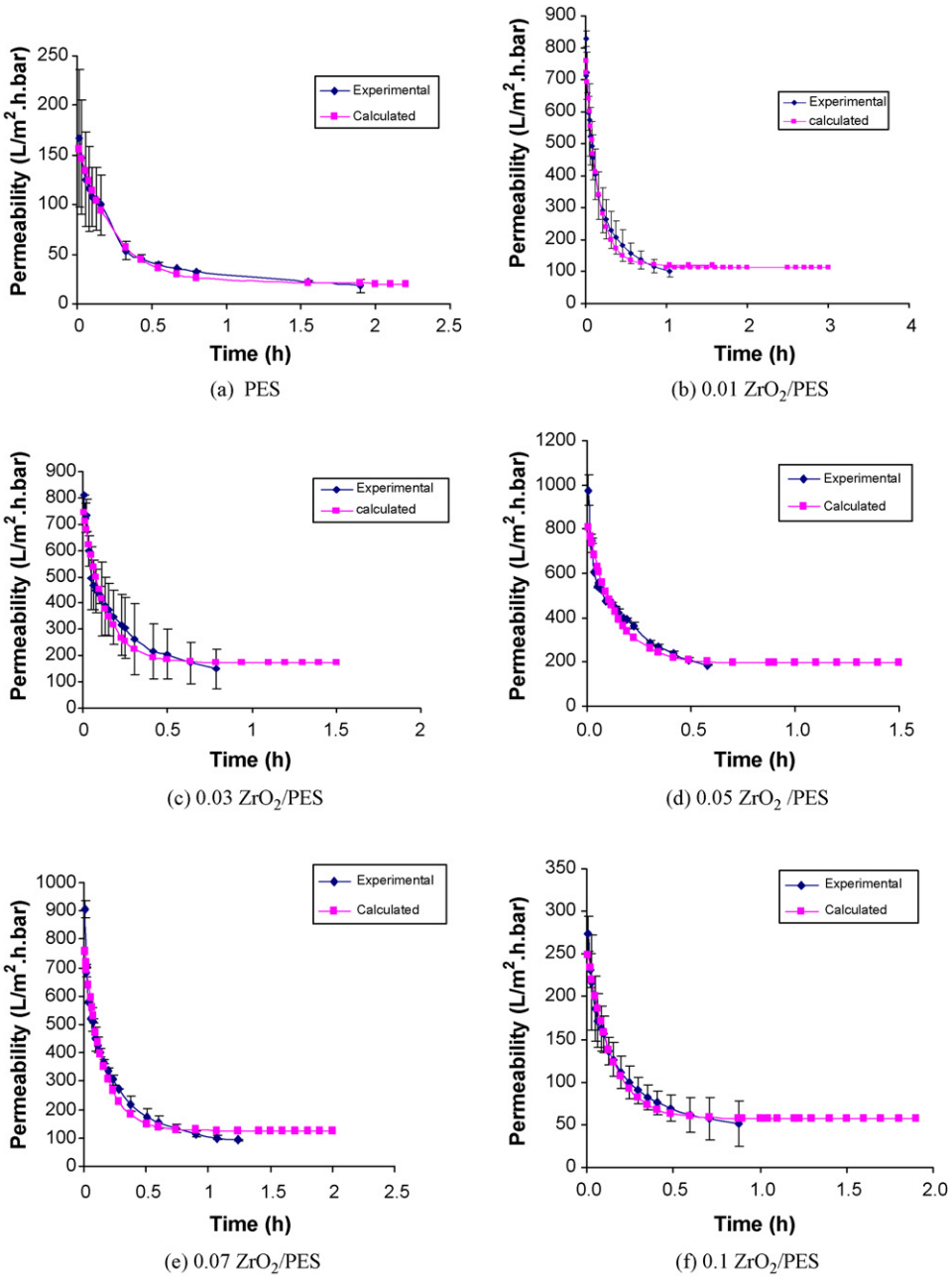

Fig. 7. Membrane permabilities: (a) PES, (b) 0.01 ZrO_2/PES, (c) 0.03 ZrO_2/PES, (d) 0.05 ZrO_2/PES, (e) 0.07 ZrO_2/PES and (f) 0.1 ZrO_2/PES

for 0.01 ZrO_2/PES to 0.96×10^7 m^{-1} for 0.1 ZrO_2/PES, were significantly different from the neat membrane (1.13×10^7 m^{-1}) at the 95% confidence level. The results clearly showed that R_c and R_t values decreased substantially with increasing ZrO_2 load up to 0.05 ZrO_2/PES membranes after which both R_c and R_t start to increase again, The differences in R_c and R_t values observed for the membranes with ZrO_2 load of 0.03 and up to 0.07 coupled with the insignificant differences observed between the R_m values and also the insignificant differences between R_f values for the aforementioned ZrO_2 loads at 95% confidence level suggest that introducing the ZrO_2 particles at these loads might affect PES membrane hydrophilicity. This is further supported by the strong linear statistical correlations (Table 4) with R of 0.89 and 0.97 observed between membrane steady-state fouling rate and both membrane total resistance (R_t) and cake resistance (R_c), respectively. As apparent from Fig. 8, the R_c values for all tested membranes ranging between 6.2×10^7 m^{-1} for PES and 1.1×10^7 m^{-1} for 0.05 ZrO_2/PES are much higher than the R_f and R_m values. This observation

Table 5
Initial and pseudo-steady-state fouling rates.

Parameters	PES	0.01 ZrO_2/PES	0.03 ZrO_2/PES	0.05 ZrO_2/PES	0.07 ZrO_2/PES	0.1 ZrO_2/PES
Initial fouling rate (L/m^2 bar h^2)	526.2	3710	3459	3907	3594	1172
Pseudo-steady-state fouling rate (L/m^2 bar h^2)	0.005	2.34E−05	2.72E−05	8.9E−06	3.71E−05	1.04E−05
Pseudo-steady-state permeability (y°) (L/m^2 h bar)	20.4	120	121.3	194.9	124.9	56.6

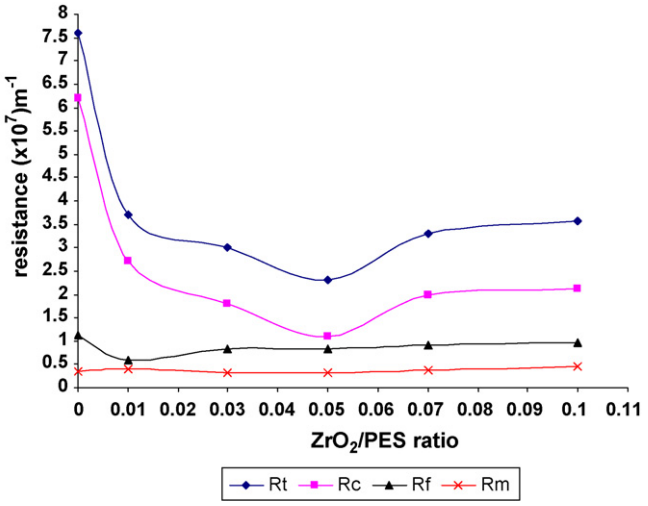

Fig. 8. Filtration resistance of neat and ZrO_2 entrapped membranes.

coupled with a direct statistical correlation ($R = 0.86$) between membrane total resistance (R_t) and cake resistance (R_c) and the reverse correlation ($R = 0.83$) between membrane steady-state permeability and cake resistance (R_c) (Table 4), suggests that the main fouling mechanism for all tested membranes was the cake layer formation. The lower R_c values observed for all tested ZrO_2/PES membranes relative to that for the PES control, coupled with the fact that cake resistance mainly due to extracellular polymeric resistance (EPS) [47] proved to be the predominant fouling mechanism suggests that introducing the ZrO_2 particles may decrease the adhesion or the adsorption of the EPS on the membrane surface. Within the 0.01, 0.03, 0.05, 0.07 and 0.1 ZrO_2/PES membranes, as discussed before in Section 3.3, introduction of ZrO_2 particles to PES membrane matrix could have two contradicting effects by increasing the solvent diffusion velocity from the membrane matrix to the water bath during the phase inversion process leading to an increase in pore size and porosity of the membrane and also by increasing membrane surface hydrophilicity which will enhance performance for sludge filtration. On the other side, the ZrO_2 particles may also block some membrane pores leading to a decrease in water flux. Despite comparable characteristics between the 0.03 and 0.05 ZrO_2/PES membranes (i.e., membrane thickness, maximum TMP, DIW permeability), the lower particle density for the 0.05 ZrO_2/PES membranes of 0.277 particle/μm^2 may be advantageous to their performance with respect to filtration resistances and fouling rate. Among the five tested ZrO_2 loads, the 0.05 was deemed to be the optimum load, despite a comparable steady-state fouling rate observed for all ZrO_2 loads, as it possesses higher DIW flux and steady-state permeability, and lower steady-state fouling rate, lower R_t, lower R_c as well as comparable R_m and R_f values among other tested ZrO_2/PES membranes.

4. Conclusions

This research aimed to investigate the role of zirconium oxide particles, with an average particles size of 221 nm, in membrane fouling mitigation for sludge filtration. ZrO_2 entrapped PES UF membranes were prepared by the phase inversion process and applied to activated sludge filtration. Major findings from this study are:

1. The addition of ZrO_2 particles to the casting PES solution enhances the membrane strength as reflected by the higher maximum TMP sustained by ZrO_2/PES membranes; however, it slightly affects other membrane physical characteristics such as membrane thickness.
2. The PES performance during sludge filtration as well as the DIW permeation was changed by the ZrO_2 particles addition. The ZrO_2 entrapped membranes showed lower flux decline, total resistance (R_t), cake resistance (R_c), and fouling resistance (R_f) compared to neat polymeric membrane, with the pseudo-steady-state permeability increasing by 3–10 folds.
3. Although fouling mitigation initially increased with ZrO_2 particles content, it reached an optimum limit above which pore plugging may occur resulting in changes in membrane performance. Within the 0.01, 0.03, 0.05, 0.07 and 0.1 ZrO_2/PES ratios, the 0.05 ZrO_2/PES ratio was deemed to be optimum in terms of membrane fouling mitigation.
4. For 0.01, 0.03, 0.05, 0.07 and 0.1 ZrO_2/PES membranes, cake formation is the predominant fouling mechanism with a direct statistical correlation between membrane total resistance (R_t) and cake resistance (R_c)

Acknowledgement

The authors would like to thank Solvay Advanced Polymers, Alpharetta, GA, USA for supplying the PES polymer

References

[1] P. Pandey, R.S. Chauha, Membranes for gas separation, Prog. Polym. Sci. 26 (2001) 853–893.
[2] A. Bottino, C. Caparmelli, P. Piaggio, V. D'Asti, Preparation and properties of novel organic–inorganic porous membranes, Sep. Purif. Technol. 22–23 (2001) 269–275.
[3] J.M. Duval, B. Folkers, M.H.V. Mulder, G. Desgrandchamps, C.A. Smolders, Adsorbent filled membranes for gas separation. Part 1. Improvement of the gas separation properties of polymeric membranes by incorporation of microporous adsorbents, J. Membr. Sci. 80 (1993) 189–198.
[4] Z.S. Wang, T. Sasaki, M. Muramatsu, Y. Ebina, T. Tanake, L. Wang, M. Watanabe, Self-assembled multilayers of titania nanoparticles and nanosheets with polyelectrolytes, Chem. Mater. 15 (2003) 807–812.
[5] R. Molinari, M. Mungari, E. Drioli, A.D. Paola, V. Loddo, L. Palmisano, M. Schiavello, Study on a photocatalytic membrane reactor for water purification, Catal. Today 55 (2000) 71–78.
[6] R. Molinari, L. Palmisano, E. Drioli, M. Schiavello, Studies on various reactors configurations for coupling photocatalysis and membrane process in water purification, J. Membr. Sci. 206 (2002) 399–415.
[7] T.H. Bae, T.M. Tak, Effect of TiO_2 nanoparticles on fouling mitigation of ultrafiltration membranes for activated sludge filtration, J. Membr. Sci. 249 (2005) 1–8.
[8] M. Moaddeb, W.J. Koros, Gas transport properties of thin polymeric membranes in the presence of silicon dioxide particles, J. Membr. Sci. 125 (1997) 143–163.
[9] L. Yan, Y.S. Li, C.B. Xiang, S. Xianda, Effect of nano-sized Al_2O_3-particle addition on PVDF ultrafiltration membrane performance, J. Membr. Sci. 276 (2006) 162–167.
[10] D.J. Lin, C.L. Chang, F.M. Huang, L.P. Cheng, Effect of salt additive on the formation of microporous poly(vinylidene fluoride) membranes by phase inversion from $LiClO_4$/water/DMF/PVDF system, Polymer 44 (2003) 413–422.
[11] N. Maximous, G. Nakhla, W. Wan, K. Wong, Preparation, characterization and performance of Al_2O_3/PES membrane for wastewater filtration, J. Membr. Sci. 341 (2009) 67–75.
[12] R.R. Bhave, Inorganic Membranes, Synthesis, Characterization and Properties, Van Rostrnd Reinhold, New York, 1991.
[13] H.P. Hsieh, Inorganic Membranes, AIChE Symp. Ser. 84 (261) (1998) 1.
[14] S. Lanone, F. Rogerieux, J. Geys, J. Boczkowski, G. Lacroix, A. Dupont, E. Maillot-Marechal, P. Hoet, Comparative toxicity of 27 manufactured nanomaterials in human alveolar epithelial and macrophage cell lines. www.nanosafe.org/home/liblocal/docs/./O4b-1_Lanone.pdf.
[15] C. Guizard, A. Julbe, A. Larbot, L. Cot, Nanostructures in sol–gel derived materials. Application to the elaboration of nanofiltration membranes, Key Eng. Mater. 61/62 (1991) 47–56.
[16] R. Vacassy, C. Guizard, V. Thoraval, L. Cot, Synthesis and characterization of microporous zirconia powders: application in nanofiltration characteristics, J. Membr. Sci. 132 (1997) 109–118.
[17] S. Benfer, U. Popp, H. Richter, C. Siewert, G. Tomandl, Development and characterization of ceramic nanofiltration membranes, Sep. Purif. Technol. 22/23 (2001) 231–237.
[18] S. Dumon, H. Barmer, Ultrafiltration of protein solutions on ZrO_2 membranes: the influence of surface chemistry and solution chemistry on adsorption, J. Membr. Sci. 74 (1992) 289–302.

[19] J. Zhong, X. Sun, C. Wang, Treatment of oily wastewater produced from refinery processes using flocculation and ceramic membrane filtration, Sep. Purif. Technol. 32 (2003) 93–98.
[20] R.S. Faibish, Y. Cohen, Fouling-resistant ceramic-supported polymer membranes for ultrafiltration of oil-in-water microemulsions, J. Membr. Sci. 185 (2001) 129–143.
[21] J. Schaep, C. Vandecasteele, R. Leysen, W. Doyen, Salt retention of Zirfon® membranes, Sep. Purif. Technol. 14 (1998) 127–131.
[22] I. Genne, S. Kuypers, R. Leysen, Effect of the addition of ZrO, to polysulfone based UF membranes, J. Membr. Sci. 113 (1996) 343–350.
[23] A. Bottino, G. Capannelli, A. Comite, Preparation and characterization of novel porous PVDF–ZrO_2 composite membranes, J. Desalination 146 (2002) 35–40.
[24] I. Genne, W. Doyen, W. Adriansens, R. Leysen, Organo-mineral ultrafiltration membranes, Filtr. Sep. 34 (1997) 964–966.
[25] T. Matsuura, Synthetic Membranes and Membrane Separation Processes, CRC Press, Boca Raton, FL, 1994.
[26] C. Buzea, I. Blandino, K. Robbie, Nanomaterials and nanoparticles: sources and toxicity, Biointerphases 2 (4) (2007) MR17–MR1721.
[27] K.J. Kim, A.G. Fane, R. Ben Aim, M.G. Liu, G. Joansson, I.C. Tessaro, A.P. Broek, D. Bargeman, A comparative study of techniques used for porous membrane characterization: pore characterization, J. Membr. Sci. 87 (1994) 35–46.
[28] X. Zheng, J. Liu, Dyeing and printing wastewater treatment using a membrane bioreactor with a gravity drain, Desalination 190 (2006) 277–286.
[29] X. Zheng, J.X. Liu, Optimizing of operational factors of a membrane bioreactor with gravity drain, Water Sci. Technol. 52 (2005) 409–416.
[30] B. Fan, X. Huang, Characteristics of a self-forming dynamic membrane coupled with a bioreactor for municipal wastewater treatment, Environ. Sci. Technol. 36 (2002) 5245–5251.
[31] S. Arabi, G. Nakhla, Impact of calcium on the membrane fouling in membrane bioreactors, J. Membr. Sci. 314 (2008) 134–142.
[32] M. Mulder, Basic Principles of Membrane Technology, Kluwer Academic Publishers, 1996, p. 383.
[33] O.V. Krasilnikov, R.Z. Sabirov, V.I. Ternovsky, P.G. Merzliak, J.N. Muratkhodjaev, A simple method for the determination of the pore radius of ion channels in planar lipid bilayer-membranes, FEMS Microbiol. Immunol. 105 (1992) 93–100.
[34] P.G. Merzlyak, L.N. Yuldasheva, C.G. Rodrigues, C.M.M. Carneiro, O.V. Krasilnikov, S.M. Bezrukov, Polymeric nonelectrolytes to probe pore geometry: application to the a-toxin trans membrane channel, J. Biophys. 77 (1999) 3023–3033.
[35] T.K. Rostovtseva, E.M. Nestorovich, S.M. Bezrukov, Partitioning of differently sized poly(ethylene glycol)s into OmpF porin, J. Biophys. 82 (2002) 160–169.
[36] H. Lee, R.M. Venable, A.D. MacKerell Jr., R.W. Pastor, Molecular dynamics studies of polyethylene oxide and polyethylene glycol: hydrodynamic radius and shape anisotropy, J. Biophys. 95 (2008) 1590–1599.
[37] M. Doi, S.F. Edwards, The Theory of Polymer Dynamics, Clarendon Press, Oxford, 1986.
[38] K. Devanand, J.C. Selser, Asymptotic-behavior and long-range interactions in aqueous-solutions of poly(ethylene oxide), Macromolecules 24 (1991) 5943–5947.
[39] C. Tanford, Physical Chemistry of Macromolecules, John Wiley & Sons, New York, 1961.
[40] M.C. Porter, Handbook of Industrial Membrane Technology, Noyes Publications, Park Ridge, NJ, USA, 1990, pp. 155–156.
[41] I.C. Kim, K.H. Lee, T.M. Tak, Preparation and characterization of integrally skinned uncharged polyetherimide asymmetric nanofiltration membrane, J. Membr. Sci. 183 (2001) 235–247.
[42] T.H. Bae, T.M. Tak, Interpretation of fouling characteristics of ultrafiltration membrane during the filtration of membrane bioreactor mixed liquor, J. Membr. Sci. 264 (2005) 151–160.
[43] S.P. Hong, T.H. Bae, T.M. Tak, S. Hong, A. Randall, Fouling control in activated sludge submerged hollow fiber membrane bioreactor, Desalination 143 (2002) 219–228.
[44] E. Tardieu, A. Grasmick, V. Geaugey, J. Manem, Hydrodynamic control of bioparticle deposition in a MBR applied to wastewater treatment, J. Membr. Sci. 147 (1998) 1–12.
[45] E. Tardieu, A. Grasmick, V. Geaugey, J. Manem, Influence of hydrodynamics on fouling velocity in a recirculated MBR for wastewater treatment, J. Membr. Sci. 156 (1999) 131–140.
[46] W.T. Lee, S.T. Kang, H.S. Shin, Sludge characteristics and their contribution to microfiltration in submerged membrane bioreactors, J. Membr. Sci. 216 (2003) 217–227.
[47] N. Maximous, S. Arabi, M. Kim, G. Nakhla, Comparison of biofoulants in BNR-MBR and conventional MBR (C-MBR) systems, in: WEFTEC Conference, McCormick Place, Chicago, IL, October 18–22, 2008.